西安交通大学
XI'AN JIAOTONG UNIVERSITY

World Scientific
www.worldscientific.com

# Grain landscape and dielectric properties of ceramics based on sodium, calcium, strontium niobates, depending on the synthesis and sintering conditions, and mechanical processing

J. Y. Zubarev[*,‡], A. V. Nazarenko[†], A. V. Nagaenko[†] and L. A. Reznitchenko[†]

*Research and Technology Unit
FGI SPA SET of the MIA RF
Rostov-on-Don, 344000, Russia

†Research Institute of Physics
Southern Federal University, 194 Stachki Ave.
Rostov-on-Don, 344006, Russia

‡yzubarev@sfedu.ru

The properties studying results of ceramics based on strontium, calcium and sodium niobates, which vary from the conditions of synthesis, sintering, and mechanical processing, are presented. The evolution of the grain structure of objects is traced depending on their phase filling during concentration changes in the composition and thermodynamic prehistory (preparation conditions).

*Keywords*: Layered perovskite-like compounds; binary systems; pyroniobates of calcium and strontium; microstructure; mechanoactivation.

## 1. Introduction

Urgent task of the last decade is the greening of all spheres of human activities, especially those related to the process of new materials for various purposes.[1] Among them, the leading position is occupied by layered structures. One of the representatives of such structures is layered perovskite-like structures based on strontium, calcium and sodium niobates.[2] The promising nature of layered media is due to the crystal-chemical specifics of their structure. Due to the mobility of interlayer cations, it is possible to change the composition of such compounds, and hence the structure.[3] The systems studies of type $(1-x)NaNbO_{3-x}Ca_2Nb_2O_7$ and $(1-x)NaNbO_{3-x}Sr_2Nb_2O_7$ were devoted to the paper,[4–6] the purpose of which was to establish the phase properties of ceramics, the extreme components of which have ultrahigh Curie temperatures: 1600 K in $Sr_2Nb_2O_7$ and 2100 K in $Ca_2Nb_2O_7$.[7,8]

## 2. Experimental

The objects of this study were ceramic solid solutions of binary systems $(1-x)NaNbO_{3-x}Ca_2Nb_2O_7(1)$ and $(1-x)-NaNbO_{3-x}Sr_2Nb_2O_7(2)$ at $0.00 \leq x \leq 1.00$; $\Delta x = 0.05$.

The solid solutions under study were prepared by a two-stage method of solid-phase reactions, at synthesis temperatures of 1220–1500 K and firing times of 4 h, followed by sintering using conventional ceramic technology at sintering temperatures, Tsp, from the interval (1530–1660) K for 2.5 h.

The mechanical activation treatment of the synthesized TP powders was carried out using an AGO-2 planetary ball mill. The compositions were loaded into drums with an inner diameter of 63 mm together with $ZrO_2$ balls 8 mm in diameter with a total weight of 200 g. The drums with the mixture were loaded into AGO-2, the powders were ground in the presence of alcohol for 10 min at a drum rotation speed of 1800 rpm.

The microstructure of solid solutions was studied using a KEYENCE VK-9700 scanning laser microscope. The light source was a 408-nm laser. The laser scanning resolution was $2048 \times 1536$ pixels with a 16-bit photomultiplier. Images of the internal structure on the cleavage of the samples were obtained with a magnification of 3000 times. Images were constructed using confocal microscopy. In this case, sequential shooting of images in focus at different heights took place. Everything that was above or below the focus was cut off by a confocal slit, while maintaining a clear only surface that was at a given height. Scanning took place from top to bottom with a step of 0.1 $\mu$m (Z-axis), after which all the images obtained at different heights were stitched together, forming a clear two-dimensional picture, and the data on the "height"

‡Corresponding author.

(i.e., the vertical position of the eyepiece) made it possible to form 3D — visualization of the investigated object without contact with its surface.

For a more detailed study of the microstructure of the samples, in particular, before and after mechanoactivation procedures, a scanning electron microscope JSM-6390L (JEOL) was used with a resolution of up to 1.2 nm at an accelerating voltage of 30 kV (image in secondary electrons), the limits of the accelerating voltage were from 0.5 to 30 kV, magnification range: from ×5 to ×300000 (beam current up to 200 nA).

## 3. Results and Discussion

Figures 1 and 2 show fragments of the microstructures of TP systems (1) and (2), including basic compounds $NaNbO_3$, $Ca(Sr)_2Nb_2O_7$. The isometric type of grain structure is characteristic of the $NaNbO_3$. Crystallites have the shape of a cube, which is displayed on the plane of the polished section by its various sections — squares, rectangles, trapezoids, triangles. The grain boundaries are generally thin, equilibrium, the packing of the structure is densely mosaic, inhomogeneous, with a spread in grain sizes from 2 $\mu$m to ~20 $\mu$m. This character of the grain landscape is preserved in both systems up to $x \sim 0.2$ (perovskite region of the PD). Further advancement into the depths of the systems as $x$ increases is accompanied by a change in the type of polycrystallinity: it becomes anisometric with acicular and plate-like grains characteristic of layered compounds. The orientation of such grains is chaotic, which is why we observe different sections of elongated prisms on the plane of the polished section. The size of the latter varies in the range (20 ÷ 30) microns (with a constant DFT of ceramics). The transition from the isometric to anisometric type of grain structure of ceramics occurs through a certain intermediate region (0.20 < $x$ < 0.25),
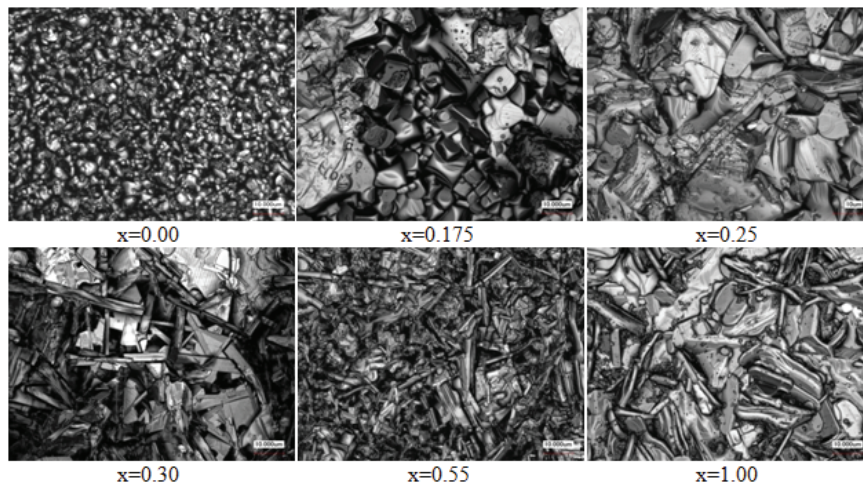


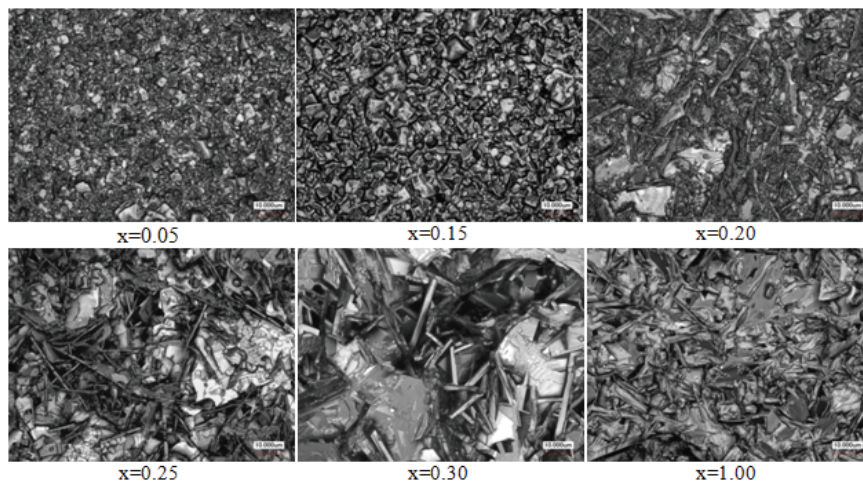Fig. 1.   Fragments of microstructures of the system $(1-x)NaNbO_{3-x}Ca_2Nb_2O_7$ (Magnification 3000).



Fig. 2.   Fragments of microstructures of the system $(1-x)NaNbO_{3-x}Sr_2Nb_2O_7$ (Magnification 3000).

the coexistence of both types of crystallites. Analysis of numerous fields of view of the same sample also showed that even far from this intermediate zone (for example, at $x \sim$ 0.10), individual acicular grains are encountered, which can be interpreted as nuclei (clusters) of a new (layered) phase, which is incipient in the depths of the perovskite field, which we previously observed in a number of ferroelectric systems with morphotropic phase transitions. The nuclei of new crystalline phases (cluster structures) are observed already far (~10–20 mol%) from the morphotropic heterophase regions, and their evolution as the concentration composition of the solid solution changes responds to the formation of macro-responses of the studied media. Since the grains habitformed during recrystallization depends on the strength and chemical bondsanisotropy.

From the existence of predominant directions of surface diffusion and self-diffusion, it can be assumed that the anisotropy of the grain growth rates in the process of primary and collective recrystallization, providing the shape and size of crystallites, which correspond to layered crystallographic symmetry, can be assumed.

Clustering of the structure and all symmetry transformations in the perovskite region are reflected in the behavior of the characteristics of the microstructure (size and shape of grains, uniformity and ordering of their packing). The same can be said about the sequence of forming layered structures accompanied by transformations of grain landscapes, which resembles "geometric" phase transitions during the formation of the microstructure of a large number of ferroelectric ceramics.

Variations of technological regulations (Figs. 3–6) have a critical impact on the nature of the microstructure of the TR of both systems. So, with an increase in DFT, a sharp increase in the average grain size is possible, and with the
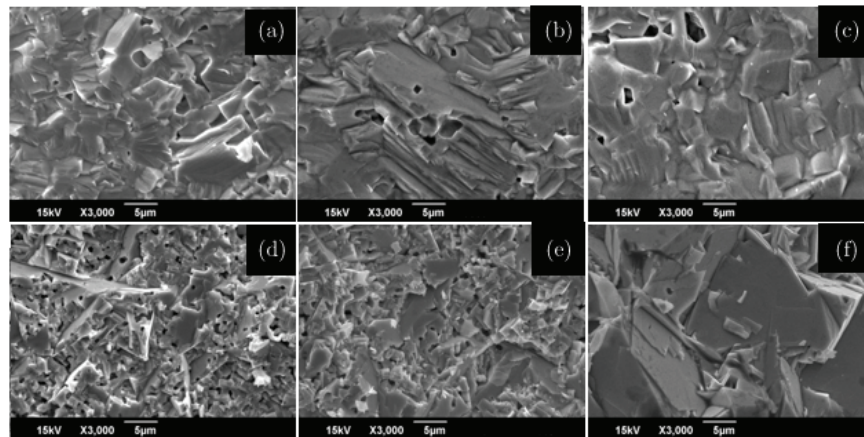


Fig. 3.  Microstructure of ceramics $(1-x)$NaNbO$_{3-x}$Ca$_2$Nb$_2$O$_7$ $x = 0.10$ (a)–(c), $x = 0.25$ (d)–(f) (a, d — 1520 K, b, e — 1570K, c, f — 1620 K) (Magnification 3000).



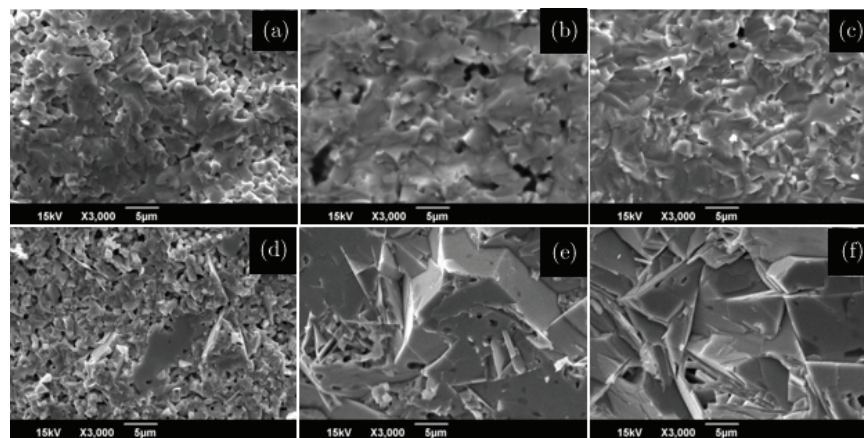Fig. 4.  Microstructure of ceramics $(1-x)$NaNbO$_{3-x}$Sr$_2$Nb$_2$O$_7$ ceramics $x = 0.10$ (a)–(c), $x = 0.25$ (d)–(f) (a, d — 1520 K, b, e — 1570 K, c, f — 1620 K) (Magnification 3000).

Fig. 5.   Microstructure of ceramics $(1-x)NaNbO_3-xCa_2Nb_2O_7$ ceramics $x = 0.10$ (a)–(c), $x = 0.25$ (d)–(f) (a, d — 1520 K, b, e — 1570 K, c, f — 1620 K) (Magnification 3000).



Fig. 6.   Microstructure of ceramics $(1-x)NaNbO_{3-x}Sr_2Nb_2O_7$ ceramics $x = 0.10$ (a)–(c), $x = 0.25$ (d)–(f) (a, d — 1520 K, b, e — 1570 K, c, f — 1620 K) (Magnification 3000).
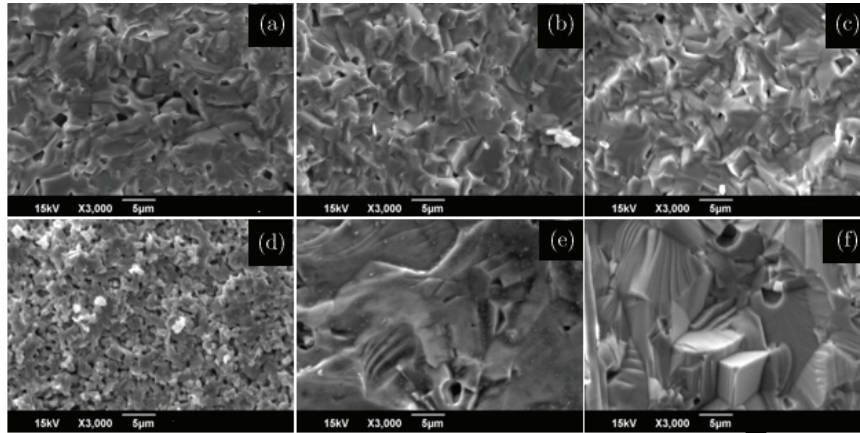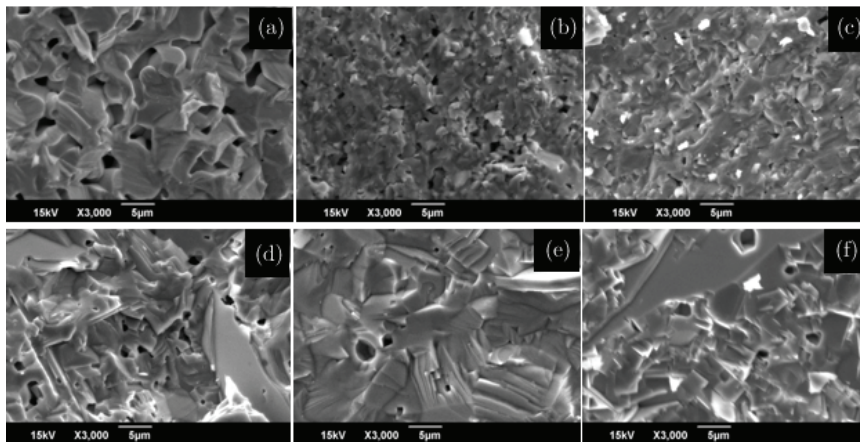
introduction of mechanoactivation procedures instead of compacting the workpieces, some loosening of the structure of ceramics was observed (especially in the "layered" region), which is probably associated with dispersion effects that cause the breakdown of materials along cleavage planes layered structures.

Optimization of the conditions for the preparation of the studied objects, it was possible to obtain ceramics with a relative density of more than 90% of the theoretical, which is the limit for the selected technology (Table 1).

The results of the study of dielectric properties are shown in Figs. 7–10.

As can be seen in the figures, an increase in $x$ in both systems leads to a decrease in $\varepsilon/\varepsilon_0$, stabilization of its thermofrequency behavior in a sufficiently wide range of temperatures and frequencies, with a smearing of the transition to the paraelectric state.

Table 1. Densities of objects before and after mechanical.

| | Non-mechanically activated objects | | |
|---|---|---|---|
| $T_{SN}$ | 1520 | 1570 | 1620 |
| Density | $\rho_{meas}$,g/cm$^3$ | $\rho_{meas}$,g/cm$^3$ | $\rho_{meas}$,g/cm$^3$ |
| (1) $x = 0.10$ | 4.46 | 4.48 | 4.49 |
| (2) $x = 0.10$ | 4.37 | 4.44 | 4.5 |
| (1) $x = 0.25$ | 4.15 | 4.31 | 4.44 |
| (2) $x = 0.25$ | 4.22 | 4.39 | 4.39 |
| | Mechanically activated objects | | |
| (1) $x = 0.10$ | 4.32 | 4.5 | 4.51 |
| (2) $x = 0.10$ | 3.89 | 4.47 | 4.44 |
| (1) $x = 0.25$ | 3.85 | 4.59 | 4.61 |
| (2) $x = 0.25$ | 4.31 | 4.45 | 4.45 |
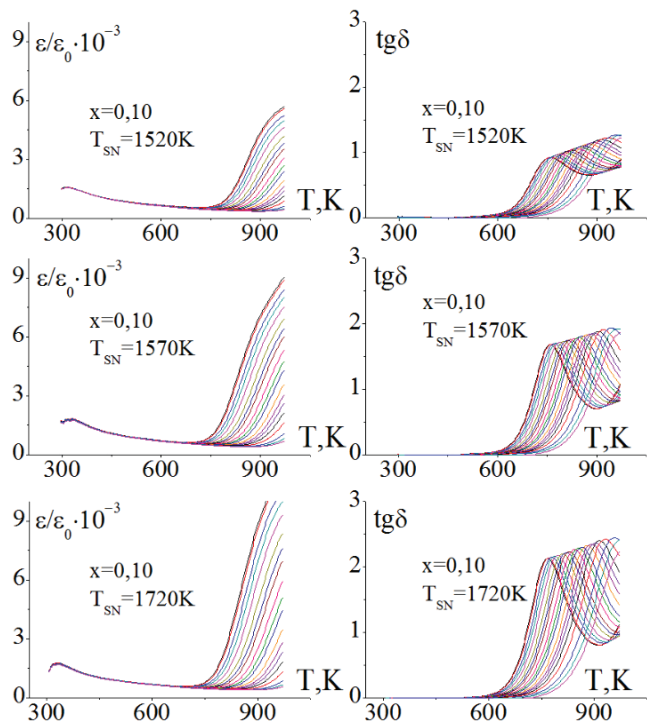
Fig. 7.    Spectra of dielectric constant $\varepsilon/\varepsilon_0$ and dielectric loss tangent tg$\delta$ system $(1-x)$NaNbO$_3$–$x$Ca$_2$Nb$_2$O$_7$.
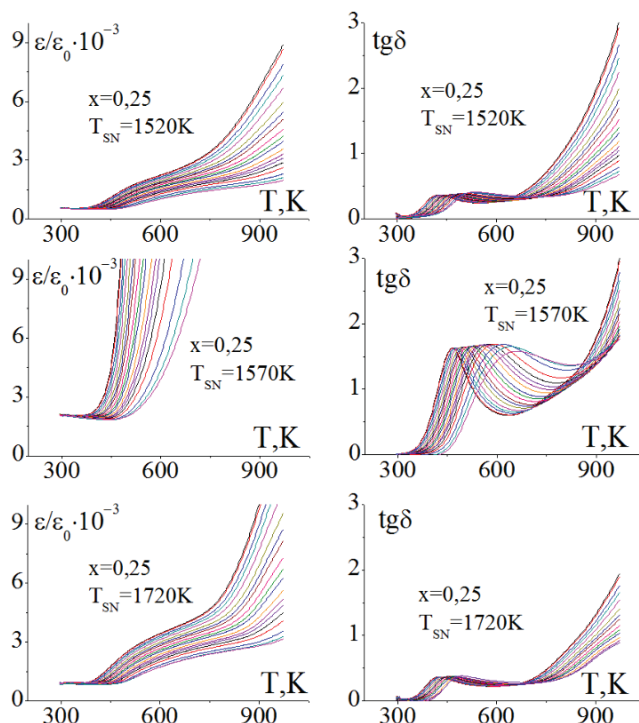
Fig. 9.    Spectra of dielectric constant $\varepsilon/\varepsilon_0$ and dielectric loss tangent tg$\delta$ system $(1-x)$NaNbO$_3$–$x$Ca$_2$Nb$_2$O$_7$.
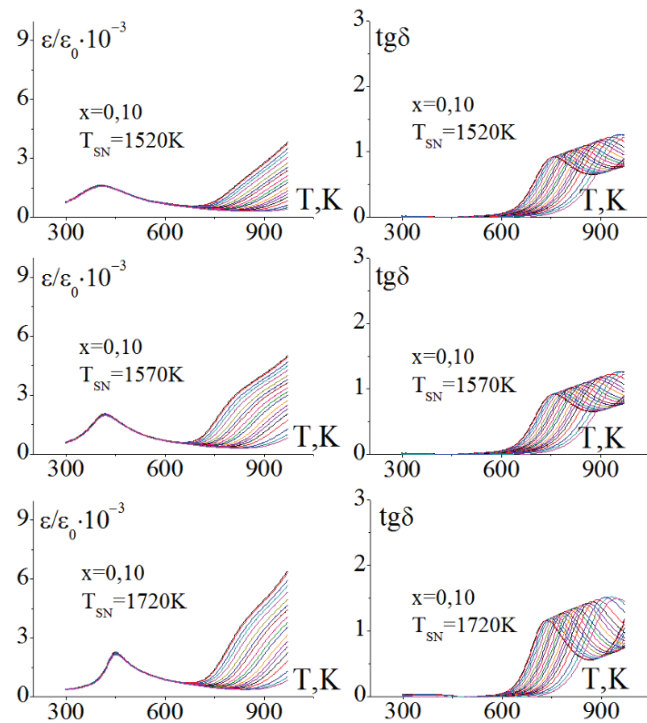
Fig. 8.    Spectra of dielectric constant $\varepsilon/\varepsilon_0$ and dielectric loss tangent tg$\delta$ system $(1-x)$NaNbO$_3$–$x$Sr$_2$Nb$_2$O$_7$.
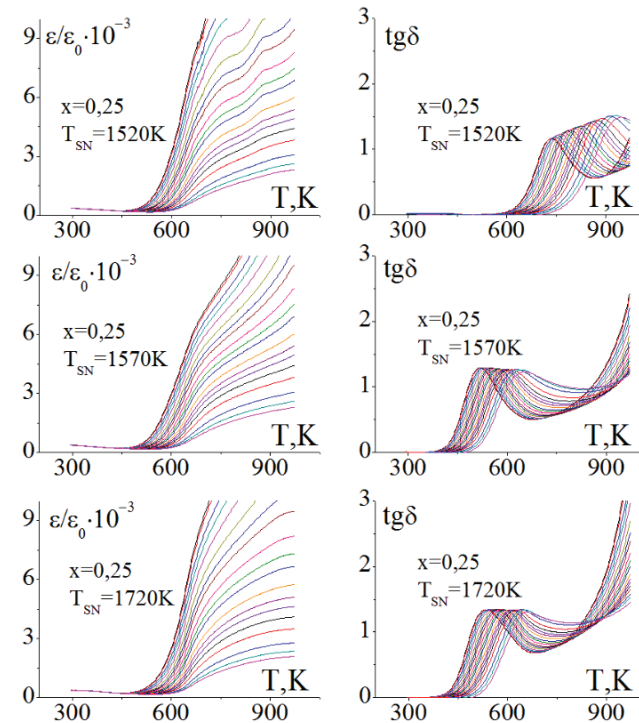
Fig. 10.    Spectra of dielectric constant $\varepsilon/\varepsilon_0$ and dielectric loss tangent tg$\delta$ system $(1-x)$NaNbO$_3$–$x$Sr$_2$Nb$_2$O$_7$.

## 4.  Conclusion

The microstructure, density and dielectric properties of ceramics based on strontium, calcium and sodium niobates were studied, depending on the conditions of synthesis, sintering and mechanical processing. The evolution of the grain structure of objects is traced depending on their phase filling at concentration changes in the composition and thermodynamic prehistory (preparation conditions). In both systems, an increase in $x$ leads to a decrease in $\varepsilon/\varepsilon_0$ and stabilization in a wide range of temperatures and frequencies.

## Acknowledgments

## References

[1]K. Chiba, N. Ishizawa and S. Oishi, A Ruddlesden–Popper-type layered perovskite, $Na_2Ca_2Nb_4O_{13}$, *Acta Cryst.* **55**, 1041 (1999).

[2]J. Y. Zubarev, L. A. Shilkina and L. A. Reznichenko, Phase states and dielectric properties of solid solutions of $(1-x)NaNbO_{3-x}Sr_2Nb_2O_7$, $(1-x)NaNbO_{3-x}Ca_2Nb_2O_7$ Binary Systems. *Bull. RAS Phys.* **80**(11), 1361 (2016).

[3]H. Ning, H. Yan and M. J. Reece, Piezoelectric stronrium niobate and calcium niobate ceramics with super-high curie points, *J. Am. Ceram. Soc.* **93**, 1409 (2010).

[4]A. Nakamura, O. Tomita, M. Higashi, S. Hosokawa, T. Tanaka and R. Abe, Solvothermal synthesis of $Ca_2Nb_2O_7$ fine particles and their high activity for photocatalytic water splitting into $H_2$ and $O_2$ under UV light irradiation, *Chem. Lett.* **44**(3), 1001 (2015).

[5]J. Yang, M. Zhao, M. Shahid, J. Feng, C. Wan and W. Pan, Electronic structure, anisotropic elastic and thermal properties of monoclinic $Ca_2Nb_2O_7$, *Ceram. Int.* **42**, 9426 (2016).

[6]R. Muhammad, Y. Iqbal and C. R. Rambo, Structure–property relationship in $NaCa_4B_5O_{17}$ (B=Nb, Ta) perovskites, *J. Mater. Sci. Mater. Electron.* **26**, 2161 (2015).

[7]J. Zubarev, N. Boldyrev, S.-H. Chang, C. Lin, A. Pavlenko, A. Nazarenko, A. Nagaenko, Y. Yurasov, I. Verbemko, I. Parinov and L. Reznichenko, Phase states, microstructure and dielectric characteristics of solid solutions $(1-x)NaNbO_{3-x}Ca_2Nb_2O_7$ and $(1-x)NaNbO_{3-x}Sr_2Nb_2O_7$, *Heliyon* **6**, e05197-1 (2019).

[8]S. Nanamatsu and M. Kimura, Ferroelectric properties of $Ca_2Nb_2O_7$ single crystal, *J. Phys. Soc. Jpn.* **36**, 1495 (1974).